Journal of Fluorescence, Vol. 9, No. 3, 1999

The Orientation of the Phosphorescence Dipole Moment of Erythrosine B Within Its Molecular Frame

M. P. Lettinga,[1,3] E. M. Klarenbeek,[1] Han Zuilhof,[2] and M. A. M. J. van Zandvoort[1]

Received August 7, 1998; accepted February 9, 1999

For an unequivocal interpretation of time-resolved phosphorescence depolarization measurements on dye molecules in biophysical systems, the orientation of the transition dipole moments within the frame of the dye has to be known. The goal of this work is to find the orientation of the phosphorescence dipole moment of erythrosine B within its molecular frame. To this end, we first determine four difference angles, exciting a molecule in two of its absorption bands and measuring the fluorescence and phosphorescence anisotropy for each excitation wavelength. The next step is to position the transition dipole moments within the molecular frame, combining the results of angle-resolved fluorescence depolarization measurements with the measured difference angles. It is shown that the phosphorescence dipole moment is tilted out of the plane of the molecule. Additionally, we find that the phosphorescence dipole moment is located above the fluorescence dipole moment and *not* above the absorption dipole moment. This induces an extra difference angle between the absorption and the phosphorescence dipole moments which in the past has been interpreted erroneously as a larger tilt out of the plane of the molecule.

KEY WORDS: Phosphorescence; transition dipole moments; erythrosine.

INTRODUCTION

Optical techniques have conveniently been used to study the orientational order and rotational dynamics of dyes incorporated in biological systems [1]. Fluorescence depolarization experiments have been performed in the studies of lipid membranes [2,3] and muscle fibers [4]. In this paper our attention is focused on the time-resolved phosphorescence anisotropy (TPA) technique, which is a powerful tool in the study of rotational dynamics on the microsecond to millisecond time scale [5]. It has been used to obtain information about membrane proteins [6–8], muscle contraction [9–11], and protein gel systems [10–12].

Depolarization experiments on dye molecules monitor the behavior of the system in which they are incorporated only indirectly. The depolarization effects arise from the change in the orientation between the absorption and the emission dipole moments of the dye during the excited state. This change is determined by three independent factors: (1) the orientation and rotation of the system to which the dye is attached, (2) the orientation and rotation of the dye molecule within this system, and (3) the orientation of the absorption and emission dipole moments within the molecular frame. Many parameters enter the analysis of the experimental data, some of which depend

[1] Debye Institute, Section of Molecular Biophysics, Utrecht University, Buys Ballot Laboratory, Princetonplein 5, 3584 CC, Utrecht, The Netherlands.

[2] Laboratory of Organic Chemistry, Wageningen University, Dreijenplein 8, 6703 HB Wageningen, The Netherlands.

[3] To whom correspondence should be addressed.

[4] *Abbreviations used:* AFD, angle-resolved fluorescence depolarization; DMF, dimethylformamide; DMSO, dimethylsulfoxide; Ery B, erythrosine B; NC, nitrocellulose; PMMA, polymethylmethacrylate; PMT, photomultiplier tube; PVA, polyvinylalcohol; TPA, time-resolved phosphorescence anisotropy.

1053-0509/99/0900-0265$16.00/0

solely on the properties of the dye. If a *priori* knowledge about these properties is not available, the interpretation of the experiment will contain many ambiguities.

One of such molecular properties is the difference angle between the absorption and the emission dipole moment, characterized by the fluorescence or phosphorescence anisotropy at the time of excitation. This so-called zero-time anisotropy is often determined in a separate experiment, using matrices to immobilize the dyes within the luminescing time scale [6,12,15,16]. In such matrices the anisotropy is constant in time and thus the anisotropy is at any time equal to the zero-time anisotropy. Knowledge of the zero-time anisotropy is of particular importance for the interpretation of phosphorescence experiments on biological systems, since in such systems the dye might have rotated within the dead time of the experiment. It has, however, been shown that the mere knowledge of the anisotropy at t-0 does not suffice to circumvent ambiguities in the interpretation. This problem has been addressed in studies on oriented systems such as crossbridges in a muscle fiber [17] and in time-resolved anisotropy measurements [18]. It was shown in these studies that the difficulties in the analysis of depolarization experiments can be overcome if the missing information about the absolute orientation of the transition dipole moments within the frame of the dye is determined in a separate experiment.

As far as the orientation of the absorption and fluorescence dipole moments is concerned, the angle-resolved method can be applied, in which the steady-state fluorescence depolarization on dyes embedded in stretched polymers [19,20] is measured under various angles. With this method the orientations of the transition dipole moments of eosin-5-maleimide [20], chlorophyll a and b [21], and 5-iodoacetamidotetramethylrhodamine [22] have been found. The orientations of the fluorescence transition dipole moments of another important dye, erythrosine, have not been determined yet. Furthermore, since this dye is of particular importance in phosphorescence depolarization experiments, the orientation of the phosphorescence dipole moment deserves special attention.

The goal of this work is thus to find the orientation of the phosphorescence dipole moment of Ery B^4 within its molecular frame. We show that in order to find this orientation, a combination of TPA measurements on an unstretched polymer film and AFD measurements on a stretched polymer film suffices. The first step in our present study is therefore the determination of the phosphorescence and fluorescence anisotropies, using the two excitation wavelengths of the Nd:YAG laser. The second step is to position the excitation and fluorescence dipole moments in the molecular frame, using the results of AFD measurements. Finally, combining the results of step 1 and step 2, the phosphorescence dipole moment can be positioned in the frame of the dye.

Following this procedure the interesting phenomenon of the assumed tilt of the phosphorescence dipole moment out of the plane of the molecule [16,23] is addressed. It is shown that the phosphorescence transition dipole moment of Ery B is indeed tilted out of the plane of the xanthene ring structure (which from now on is called the plane of the molecule). Such a tilt was predicted and partly measured in earlier research [16]. However, the tilt out of the plane is less than expected, since there is also a tilt from the plane normal to the molecular plane along the inertial axis. The latter tilt was never noticed, because in earlier studies just one excitation wavelength was used.

Having determined the orientation of the phosphorescence transition dipole moment within the molecular frame, phosphorescence depolarization measurements in other systems can be interpreted in terms of the dynamics of the system of interest, independent of the properties of the dye molecule.

THEORY

Luminescence Anisotropy of Molecules in Immobilized Solutions

The geometry for luminescence anisotropy measurements is shown in Fig. 1. The sample is illuminated with vertically (V) polarized light, while the emitted light is detected with horizontal (H) or vertical (V) polarization in a direction perpendicular to the excitation beam. The anisotropy r is then defined by

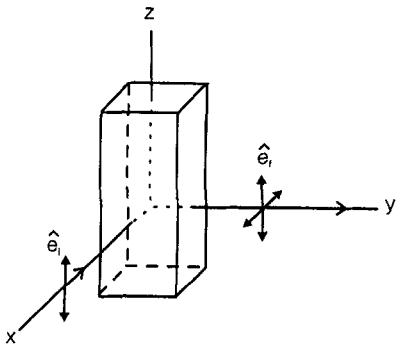

Fig. 1. Setup for anisotropy experiments. The excitation light is vertically polarized ($\hat{e}_i$), while the emitted light is either horizontally or vertically polarized ($\hat{e}_f$).

$$r = \frac{I_{VV} - I_{VH}}{I_{VV} + 2I_{VH}} \quad (1)$$

In this equation the subscripts denote the polarization directions of the exciting and emitted light, respectively, in the laboratory frame.

If the dye molecules are randomly distributed in the sample, the anisotropy and its decay after a short light pulse will be determined by the difference angle Δ between the absorption and the emission dipole moments within the molecular frame and by the rotational dynamics of the dye molecules [24]. In its most general form the anisotropy can be written as a sum of exponentials [25,26],

$$r(t) = r(0) \sum_i a_i e^{-t/\varphi_i} \quad (2)$$

where $r(0)$ is the anisotropy at $t = 0$,

$$r(0) = \frac{2}{5}\{3(\cos\Delta)^2 - 1\} \quad (3)$$

and φ_i are the typical decay times. If, furthermore, the dye molecules are immobilized within the time scale of the luminescing process $\varphi_i \rightarrow \infty$ and thus the anisotropy is constant in time and equals $r(0)$. In the latter case the steady-state experiment suffices to determine the difference angle Δ since $r_{ss} = r(0)$.

Thus, anisotropy experiments on unstretched polymer films yield the difference angle between the absorption and the emission dipole moments within the molecular frame. Because the absorption process is independent of the emission process, Eq. (2) holds for both fluorescence and phosphorescence.

Combining Phosphorescence and Fluorescence Anisotropies

As explained in the previous section, the difference angle between absorption and emission dipole moments can be found using anisotropy measurements on randomly oriented and immobilized dye molecules. Thus, by exciting a molecule in two separated absorption bands and measuring for each excitation both the fluorescence anisotropy and the phosphorescence anisotropy, four difference angles are found. The angles between the two absorption dipole moments and the fluorescence dipole moments is called ε_{355}, respectively, ε_{532}. The angles between the two absorption dipole moments and phosphorescence dipole moments is called δ_{532}, respectively, δ_{532}. The index indicates the excitation wavelength. In the following it is tacitly assumed that all difference angles are smaller than 90°.

The anisotropy experiment does not yield any information on the difference angle between the two absorption dipole moments ($\Delta\mu$). However, assuming that the absorption and fluorescence dipole moments are located in the plane of the molecule [27,28], there are only two possible ways of positioning the two absorption dipole moments with respect to the fluorescence dipole moment: (1) the absorption dipole moments $\vec{\mu}_{355}$ and $\vec{\mu}_{532}$ are positioned at the same side of the fluorescence dipole moment $\vec{\nu}_{flu.}$, so $\Delta\mu$ is given by $\varepsilon_{355} - \varepsilon_{532}$; or (2) $\vec{\nu}_{flu}$ is positioned between $\vec{\mu}_{355}$ and $\vec{\mu}_{532}$, so $\Delta\mu$ is given by $\varepsilon_{355} + \varepsilon_{532}$.

For the two situations knowledge of the difference angles now yields a distinct orientation of the phosphorescence dipole moment with respect to the absorption and fluorescence dipole moments (see Fig. 2). If $\varepsilon_{355} + \varepsilon_{532} \neq \delta_{355} + \delta_{532}$ (or $\varepsilon_{355} - \varepsilon_{532} \neq \delta_{355} - \delta_{532}$), the only possible way to produce a consistent picture of the relative positions of the transition dipole moments is to tilt the phosphorescence dipole moment out of the plane of the molecule. The concept that the phosphorescence dipole moment is tilted out of this plane is not new [23],

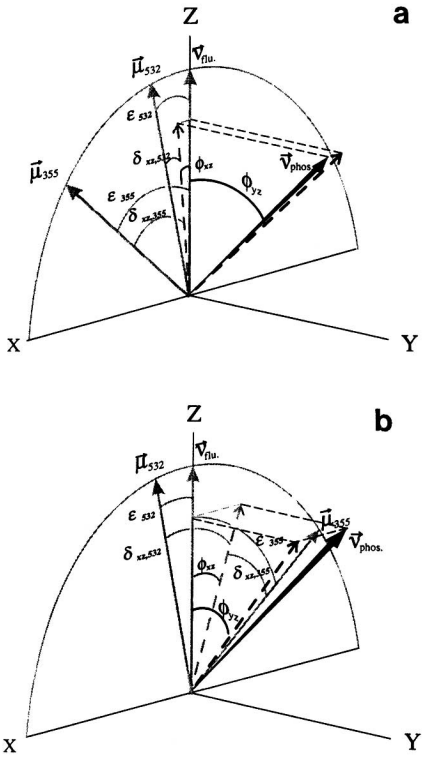

Fig. 2. Determination of the orientation of the phosphorescence dipole moment using fluorescence and phosphorescence anisotropies. The dashed arrows are the projections of the phosphorescence dipole moment on the *xz*- and *yx*-plane. The difference angle between the two absorption dipole moments ($\Delta\mu$) is given by (a) $\varepsilon_{355} - \varepsilon_{532}$ and (b) $\varepsilon_{355} + \varepsilon_{532}$.

however, the angle of the tilt has never been determined accurately. We show below that the exact tilt strongly depends on the choice between case 1 and case 2.

In the following we place the xz-plane in the plane of the molecule, where the z axis is defined as the longer axis of the xanthene ring structure. For convenience, the fluorescence dipole moment will be positioned along this axis. We introduce δ_{xz355} and δ_{xz532} as the angle between the respective absorption dipole moments and the projection of the phosphorescence dipole moment on the xz-plane. φ_{yz} is defined as the angle between the projection of $\vec{\nu}_{phos}$ on the yz-plane and the z-axis and, therefore, gives the tilt between the phosphorescence dipole moment and the plane of the molecule. Because φ_{yz} does not depend on the excitation wavelength, δ_{355} can be separated in φ_{yz} and δ_{xz532}, and δ_{532} can be separated in φ_{yz} and δ_{xz355} (see Figure 2). φ_{yz} can now be written as

$$\varphi_{yz} = \frac{\cos\delta_{532}}{\cos\delta_{xz532}} = \frac{\cos\delta_{355}}{\cos\delta_{xz355}} \tag{4}$$

In case 1 the difference angle between the two absorption dipole moments is given by

$$\Delta\mu = \varepsilon_{355} - \varepsilon_{532} = \delta_{xz355} - \delta_{xz532} \tag{5}$$

remembering that the emission process is independent from the excitation process.

Eliminating φ_{yz} and δ_{xz355}, we find for δ_{xz532}

$$\delta_{xz532} = \tan^{-1}\left\{\left(\cos\Delta\mu - \frac{\cos\delta_{355}}{\cos\delta_{532}}\right)\Big/\sin\Delta\mu\right\} \tag{7}$$

All parameters on the right side of the equation are known, and therefore δ_{xz532} can be calculated. Now, using Eq. (4), can φ_{yz} also be found.

In case 2, $\Delta\mu$ is given by

$$\Delta\mu = \varepsilon_{355} + \varepsilon_{532} = \delta_{xz355} + \delta_{xz532} \tag{8}$$

yielding

$$\delta_{xz532} = \tan^{-1}\left\{\left(\frac{\cos\delta_{355}}{\cos\delta_{532}} - \cos\Delta\mu\right)\Big/\sin\Delta\mu\right\} \tag{9}$$

If the two absorption dipole moments are mutually orthogonal, both situations yield the same difference angle δ_{xz532}. However, it has been shown that even for highly symmetric molecules, the absorption and fluorescence dipole moments are not necessarily mutually orthogonal [2,20,21].

Thus, combining phosphorescence and fluorescence anisotropies, two distinct orientations of the phosphorescence dipole moment relative to the absorption and fluorescence dipole moments are found, depending on the position of the emission dipole moment relative to the two absorption dipole moments (case 1 and 2, respectively). In the next section we show how the orientations of the absorption and fluorescence dipole moments can be related to the inertial axis of the molecule, using angle-resolved fluorescence depolarization (AFD) measurements. With this knowledge we will be able to make a choice between case 1 and case 2.

AFD Theory

From an anisotropy experiment on a randomly oriented sample, only the difference angle between the absorption and the emission dipole moment can be extracted. The orientation of the transition dipole moments within the molecular frame can be determined applying the AFD method [19,20]. In this experiment, the dyes are macroscopically aligned and immobilized in a stretched polymer film and illuminated with horizontally polarized light (H), varying the angle of incidence, θ. Horizontally (H) and vertically (V) polarized fluorescence light is detected, varying the detection angle, ϕ. The geometry of the AFD experiment is shown in Fig. 3. Under these experimental conditions the fluorescence intensities I_{HH} and I_{HV} and their ratio $R_e(=I_{HV}/I_{HH})$ are given by the following expressions [18,24]:

$$\begin{aligned} I_{HV} &= (k/9)(1 + 2S_\mu - S_\nu - 2G_0 \\ &\quad - 3(S_\nu - G_0 + G_2)\sin^2\theta) \\ I_{HH} &= (k/9)(1 + 2S_\mu + 2S_\nu + 4G_0 \\ &\quad - 3(S_\mu + 2G_0)\sin^2\theta - (S_\nu + 2G_0)\sin^2\phi \\ &\quad 3(3G_0 + G_2)\sin^2\theta\sin^2\phi - 3G_1\sin2\theta\sin2\phi) \end{aligned} \tag{11}$$

The terms in this expression have the following meanings.

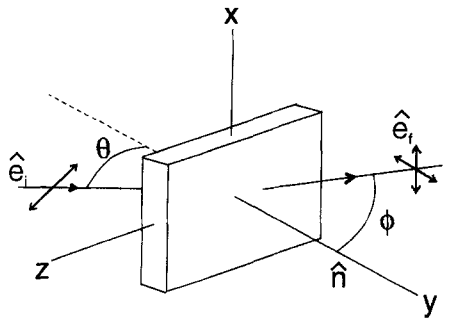

Fig. 3. Schematic view of the setup for AFD experiments on flat samples. The incoming light is horizontally polarized ($\hat{e}_i$), while the emitted light is either horizontally or vertically polarized ($\hat{e}_f$). The stretching direction of the film is placed along the y-axis.

I_{IF}: The intensity of the fluorescence light with polarization direction F, caused by illuminating the sample with a light beam with polarization direction I. (See also Fig. 3.)

k: A constant determined by the excitation light intensity and probe concentration.

$$S_\mu = \sum_{i=-2}^{2} \langle D_{0i}^2(\Omega_{sm})\rangle D_{i0}^2(\Omega_\mu) \tag{12}$$

$$S_\nu = \sum_{j=-2}^{2} \langle D_{0j}^{2*}(\Omega_{sm})\rangle D_{j0}^{2*}(\Omega_\nu) \tag{13}$$

$$G_k = \sum_{i,j=-2}^{2} \langle D_{kj}^{2*}(\Omega_{sm}) D_{ki}^2(\Omega_{sm})\rangle D_{j0}^{2*}(\Omega_\nu) D_{i0}^2(\Omega_\mu) \tag{14}$$

$D_{mn}^L(\Omega)$: Wigner rotation matrix element [29].

$\Omega_\mu(\alpha_\mu, \beta_\mu, \gamma_\mu)$ Euler angles of the absorption dipole moments within the molecular frame.

$\Omega_\nu(\alpha_\nu, \beta_\nu, \gamma_\nu)$ Euler angles of the emission dipole moments within the molecular frame.

Ω_{sm} Euler angle between the director of the Ery B molecule and the director of the film.

$\langle X_{sm}\rangle$ The ensemble average $\int d\Omega_{sm} f(\Omega_{sm}) X(\Omega_{sm})$ of $X(\Omega_{sm})$ over the distribution function $f(\Omega_{sm})$.

$f(\Omega_{sm})$ Orientational distribution function of the dye molecules.

The various angles are depicted in Fig. 4. Equation (11) expresses the separation of the geometrical factors θ and ϕ, dictated by the experimental setup, from the molecular properties, the order parameters S_μ and S_ν, and the correlation functions G_k. The correlation functions are related to the anisotropy by

$$r = 0.4 \sum_{k=-2}^{2} G_k \tag{15}$$

In the following we limit ourselves to the case of quenched reorientational motions. We also assume the orientational distribution of the pigments in the polymer matrix to be either isotropic (in an unstretched film) or uniaxially symmetric around the stretch direction (in a stretched film) so that $G_k = G_{-k}$ [19,24,29].

Equation (11) indicates that a fluorescence depolarization experiment yields a maximum of five independent parameters, S_μ, S_ν, G_0, G_1, and G_2. These experimental parameters contain all the accessible molecular information. The question arising now is how to extract the information on orientational distribution and the transition dipole moments from the five experimental parameters.

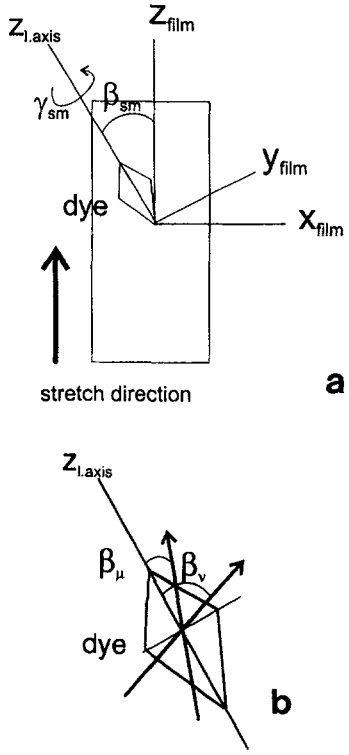

Fig. 4. Two independent orientations determine the polarization. (a) The dye molecule relative to the director of the film. $z_{l.axis}$ axis is the long axis of the dye. γ_l gives the rotation of the molecule around this long axis and $\beta_{l,d}$ gives the angle between the long axis and the director of the film. (b) The transition dipole moments relative to the inertial axis of the dye, where the index of the angles represents the transition dipole moment.

Ery B consists of a planar chromophoric xanthene system just like rhodamine, attached to a ring that is twisted 90° to the plane of the xanthene rings [32]. We can thus locate the absorption and fluorescence dipole moments in the xanthene plane. Conclusively, the absorption and fluorescence dipole moments are completely defined by the Euler angles β_μ and β_ν with the inertial axis of the chromophoric plane.

In the case of quenched reorientational motions, the correlation functions G_k can be expressed in the order parameters of rank $L = 2$ and $L = 4$, using the Clebsch Gordon series and the Euler angles of the transition dipole moments [27,29]. The orientational information in the experimental parameters (S_μ, S_ν, G_0, G_1, and G_2) is expressed in up to 25 second-rank and 81 fourth-rank order parameters. However, many of these are zero for reasons of symmetry [19,24,29]. For films stretched uni-

axially along the Z-axis, the distribution of the planar pigments is invariant under rotations around this axis, possesses mirror-symmetries in the XY- and the XZ-plane of the film, and, moreover, is invariant to reflections in the xz- and the yz-molecular frames. Consequently only five nonzero order parameters remain:

$$\langle P_2 \rangle = \langle D^2_{00} \rangle, \langle P_4 \rangle = \langle D^4_{00} \rangle, \langle D^2_{02} \rangle, \langle D^4_{02} \rangle, \text{ and } \langle D^4_{04} \rangle$$

As we need two parameters for the angles of the transition moments, there are in total seven parameters to extract from the five experimentally available parameters S_μ, S_ν, G_0, G_1, and G_2. In a polymer a good choice for the interpretation of the data is the use of the first three parameters, $\langle P_2 \rangle$ $\langle P_4 \rangle$, and $\langle D^2_{02} \rangle$. The smoothest possible orientational distribution function $f(\Omega_{sm})$ that is consistent with these three order parameters may be reconstructed with the maximum entropy formalism given by van Gurp *et al.* [18] and Levine and Bernstein [33]:

$$f(\Omega_{sm}) = Ae^{\lambda_2 P_2(\Omega_{sm}) + \lambda_4 P_4(\Omega_{sm}) + \varepsilon [D^2_{02}(\Omega_{sm}) + D^2_{0-2}(\Omega_{sm})]} \tag{16}$$

In this equation A is a normalization constant. λ_2, λ_4, and ε are variables whose values are uniquely related to the three order parameters.

Any order parameter $\langle X \rangle$ can be calculated from this equation with the above expression, since $\langle X \rangle = \int d\Omega_{sm} f(\Omega_{sm}) X(\Omega_{sm})$. This approach now expresses the five experimental parameters S_μ, S_ν, G_0, G_1, and G_2 in terms of three variables (λ_2, λ_4, and ε) describing the orientational distribution of the molecules relative to the stretch direction and two variables (β_μ and β_ν) defining the orientation of the transition dipole moments relative to the in-plane z-axis of the molecular ring, using Eqs. (12)–(14).

EXPERIMENTAL

Sample Preparation

Ery B was obtained from Sigma Chemical Co. and used without further purification. Dimethylsulfoxide (DMSO), dimethylformamide (DMF), and ethanol of analytical-grade purity were obtained from J. T. Baker chemicals B.V. and used without further purification. Spectrophotometric grade glycerol was obtained from Aldrich. Completely hydrolyzed polyvinylalcohol (PVA) with an average weight of about 100 kD was obtained from Aldrich Chemie and cleaned from side-products (acidic traces and residual acetyl groups) by the modified ethanol extraction method described by van Zandvoort *et al.* [35]. Nitrocellulose (NC) powder was obtained from Wolff Walsroder A.G. and purified before use as described by van Zandvoort *et al.* [34].

A PVA solution in DMSO was prepared under nitrogen atmosphere by adding 0.5 g cleaned PVA powder to 6 ml DMSO and heating this mixture to 80°C under continuous magnetic stirring until an optically clear solution was obtained. The PVA–DMSO solution was cooled down and then mixed with a small amount of an Ery B stock solution in DMSO. An NC solution in DMF was prepared under nitrogen atmosphere by adding 0.8 g NC to 6 ml DMF and stirring this mixture at room temperature until an optically clear solution was obtained. Then the desired amount an Ery B stock solution in DMSO was added and homogenized. The concentration of dye in the polymer film was $2 * 10^{-7}$ mol/g. This concentration was chosen in order safely to assume energy transfer processes to be absent [22].

Films for anisotropy measurements were prepared from the polymer solutions by pouring it out on a quartz plate and drying in the dark for 24 h under a continuous nitrogen stream at room temperature, followed by 3 days at 60°C. The latter procedure was followed to ensure complete evaporation of DMSO out of the polymer film. This is crucial in order to immobilize the embedded dye molecules within the phosphorescence time scale. Next, the film was covered with a droplet of glycerol for optical contact and another quartz plate. Finally, the samples were sealed at the edges with glue and taped, leaving a small hole free for illumination.

Films for the AFD measurements were prepared pouring out an NC solution on a glass plate and drying it in the dark for 40 h under a continuous nitrogen stream. A rectangular piece of film was cut from the glass plate and put in a homemade stretching bank. After leaving it in a desiccator with DMF for about 30 min, the film was stretched till it reached at least twice its original length. A piece from the center was cut and dried, after which it was pressed between quartz plates using glycerol to improve optical contact. Finally, the samples were sealed at the edges with glue and taped, leaving a small hole free for illumination. The uniaxiality of the NC films stretched in this way was checked previously by us [36] using the methods described in Refs. 24 and 37. The refractive index of both stretched and unstretched NC films and unstretched PVA films was measured with an Abbe refractometer and found to be 1.52 ± 0.02, with a birefringence within the experimental error.

Spectral Measurements

The absorption spectrum of the emission filter was measured on a Hewlett Packard 8452 A diodearray spec-

trophotometer. The phosphorescence spectra of Ery B were measured on a Perkin Elmer LS 50 B luminescence spectrometer.

The steady-state fluorescence excitation and emission anisotropy spectra on all samples were measured with a SLM-Aminco SPF 500 spectrofluorimeter with its standard anisotropy device, using 90° geometry. The detection wavelength for the excitation spectra was 565 nm and the excitation wavelength for the emission spectra was 515 nm. The correction factor (I_{HH}/I_{HV}), accounting for the difference in response of the emission line to horizontally and vertically polarized light, was determined on the Ery B/glycerol solution.

Time-Resolved Phosphorescence Setup

While from earlier experiments it is known that the dye molecules in polymer film are immobilized within the fluorescence time scale, this is not known for the phosphorescence time scale. Therefore the phosphorescence anisotropy has to be measured time-resolved, in contrast to steady-state fluorescence anisotropy measurements. For these experiments we used a Nd:YAG-laser (Continuum) as the excitation light source, running at 10 Hz.. The pulse width of the laser was 6 ns, which makes it effectively a delta pulse for the time scale at which the measurements are performed. The second (532-nm) and third (355-nm) harmonic of the laser were used to excite the molecules in its two excitation bands. The power on the sample should be kept relatively low, in order to avoid saturation of the population of excited molecules, which would result in a lower anisotropy [38, 39]. A liquid filter with potassium bichromate and a suitable setting of the Q-switch were used to reduce the laser intensity within the margins indicated by Peng and Barisas [38].

The experiments were performed with a standard 90° setup. An extra Glen–Tayler prism was used to select the vertical excitation light. For the determination of the correction factor a Soleil–Blodget was used to turn the polarization 90°. The sample is placed with the normal at an angle of 45° with the incident beam. A sheet polarizer was used to select the polarization direction of emission light. An Omega interference filter(680 nm) was used for spectral filtering of the phosphorescence light (Fig. 5).

Performing time-resolved phosphorescence experiments one has to avoid saturation of the PMT by the instant scattering and fluorescence light, which is orders of degrees more intense than the phosphorescence light. Although the phosphorescence spectrum is red-shifted relative to the fluorescence spectrum, spectral filtering does not suffice to avoid saturation of the PMT [40,41]. To this end, a home-built gating device was incorporated in to the bleeder circuit of the PMT, following the scheme of Ballard [42]. It produces a 500-ns pulse of about 200 V over the first few dynodes of the PMT. Switching noise was reduced by a careful linking of the grounding. The dead time was reduced to 300 ns.

The output of the PMT is sampled with a Lecroy 9370 digitizing oscilloscope at a maximal sampling rate of 500 Msamples/s, enabling us to detect every single photon that is captured by the PMT after the gating pulse. Sweeps containing up to $25 \cdot 10^3$ samples were summed, averaged, and stored on an internal memory card. Each experiment consisted on average of 2048 sweeps. The memory card was read by a PC every 256 sweeps.

Steady-State AFD

Steady-state AFD experiments were carried out on the setup as described by van Gurp *et al.* [24]. The excitation light was selected to be either 338 or 528 nm. The 338-nm wavelength was selected with an 338 ± 10-nm interference filter and two broadband filters. This wavelength was chosen because the absorbance at 338 nm is higher than at 355 nm (the excitation wavelength of the Nd:YAG-laser), whereas the anisotropy is the same at both wavelengths. The 528-nm wavelength was selected with a 528 ± 5-nm interference filter and a 540-nm low-pass filter. The excitation light was polarized with a horizontally aligned Glan–Taylor prism. The emission light was detected through a 573 ± 5-nm interference filter and a GG560 cutoff filter. The horizontally and vertically polarized emission light were detected using a sheet polarizer. The measurements were done for 63 angles of excitation and emission. The correction factor (I_{HH}/I_{HV}) to account for the difference in response of the emission line to horizontally and vertically polarized light was determined on the same setup in a 90° setup on a dilute solution of Ery B in ethanol.

The polarization ratios for both wavelengths were analyzed simultaneously with a global tanget approach using a nonlinear least-squares Marquard procedure. The values for λ_2, λ_4, and ε were allowed to vary, while the value for β_v was kept fixed [20,21]. The difference angles between the absorption dipole moments and the emission dipole moment were kept fixed on the values determined by the anisotropy measurement. The sign of the difference angle was left as a variable. By doing this for a sequence of fixed values of β_v, the χ^2 minima were found.

Calculation of Molecular Structure

The molecular structures were drawn in ChemOffice (CambridgeSof Corporation, Cambridge, MA 02139, USA; ChemDraw version 4.0/Chem3D version 4.5, 1997)

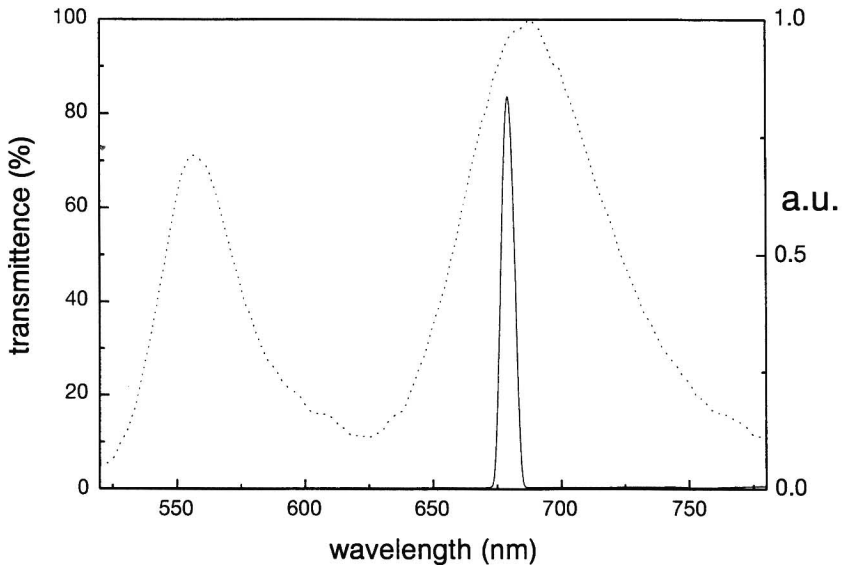

Fig. 5. Spectral selection of the phosphorescence (dotted line) by the interference filter (solid line).

and preoptimized with the MM2 force field implemented there. Subsequently, the geometry was fully optimized via PM3 computations [43], and the resulting geometries were verified to correspond to real minima on the potential energy surface via computation of the vibrational frequencies. These computations were performed on a Silicon Graphics R10000 O2 computer using MOPAC 93 [44] and MOPAC 97 programs within ChemOffice.

RESULTS

Fluorescence Anisotropy (Steady State)

The steady-state fluorescence anisotropy of Ery B has been determined in glycerol, PVA, and NC. Earlier measurements on the same type of samples showed that the dye molecules are immobilized within the fluorescence time scale. Thus, in order to determine the difference angle between the absorption and the fluorescence dipole moment, it suffices to determine r_{SS}. For both excitation wavelengths, 355 and 532 nm, it was found that the anisotropy was independent of the solvents used. The fluorescence spectra and anisotropy spectrum for Ery B in glycerol are given in Fig. 6. It can be seen in this figure that the anisotropy is the same for $\lambda_{exc} = 355$ nm as for $\lambda_{exc} = 338$ nm, being $r_{fluo.338-335} = -0.01 \pm 0.03$. At $\lambda_{exc} = 532$ nm the anisotropy equals $r_{fluo.532} = 0.38 \pm 0.01$. The values correspond with a difference angle of $\varepsilon_{355} = 55 \pm 2°$ between $\vec{\mu}_{355}$ and $\vec{\nu}_{flu}$ and of $\varepsilon_{532} = 13 \pm 2°$ between $\vec{\mu}_{532}$ and $\vec{\nu}_{flu}$.

TPA on Polymer Films

A typical measurement is depicted in Fig. 7, where the anisotropy of Ery B immobilized in a PVA film has been measured. For this experiment the same samples were used as for the fluorescence anisotropy measurements. Clearly, the anisotropy does not decay when the sample is properly dried. The $r(t = 0)$ can easily be extrapolated. Exciting at 355 nm, the phosphorescence anisotropy was $r_{phos.355} = 0.00 \pm 0.02$. Exciting at 532 nm, the phosphorescence anisotropy was $r_{phos.532} = 0.25 \pm 0.01$. These values correspond with difference angles of $\delta_{355} = 55 \pm 2°$ between $\vec{\mu}_{355}$ and $\vec{\nu}_{phos}$ and $\delta_{532} = 29 \pm 1°$ between $\vec{\mu}_{532}$ and $\vec{\nu}_{phos}$.

The anisotropies of the delayed fluorescence were also determined. It was found that they coincided with the ordinary fluorescence anisotropies.

In the 532-nm band no differences were found between the phosphorescence anisotropies measured on PVA and on NC films, implying that we can combine AFD measurements on NC films with TPA measurements on PVA films.

AFD Results

AFD measurements were performed on Ery B in NC film ($c = 2 * 10^{-7}$ mol/g), stretched to three times its original length. The polarization ratio was measured at 63 angle combinations. For each film excitation at two absorption wavelengths was used, while the fluorescence was detected at one emission wavelength. Thus, for each

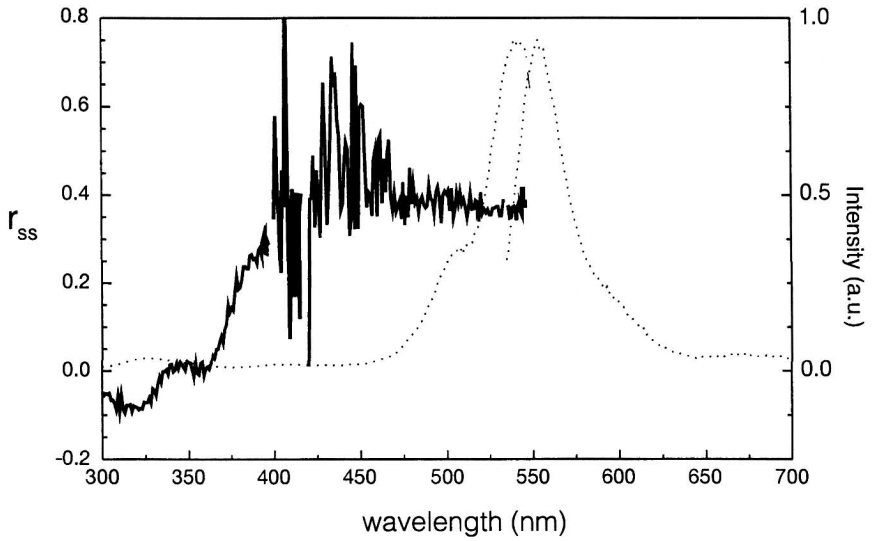

Fig. 6. Steady-state excitation and emission spectra of the fluorescence intensity (dotted lines) and fluorescence anisotropy (solid line) of Ery B in glycerol. The excitation wavelength was 515 nm. The detection wavelength was 565 nm.

film two data sets of 63 points were acquired. The two data sets were fitted simultaneously to the six adjustable parameters, while the fit parameters concerning the molecular distribution and β_ν were linked (see Experimental).

In Fig. 8 two profiles of χ^2 vs β_ν, the angle between the emission dipole moment and the z-axis of the molecule, were plotted. For one of the profiles $\beta_{\mu 1} < \beta_\nu < \beta_{\mu 2}$, while for the other $\beta_\nu < \beta_{\mu 1} < \beta_{\mu 2}$. Solutions were found from the minima in the χ^2 surface. The solutions for $\beta_{\mu 1} < \beta_\nu < \beta_{\mu 2}$ are given in table I, with the corresponding orientational distribution functions in Fig. 9. The error margins in the values of the adjustable variables were estimated from the limits in the minimum of the χ^2 profile. These errors had only a marginal effect on the features of the orientational distribution functions.

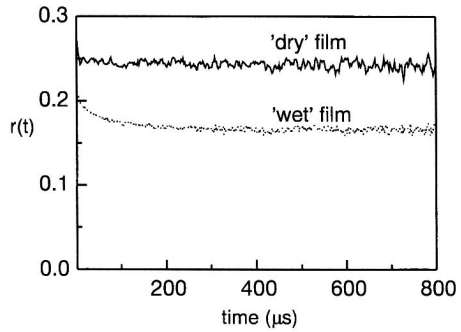

Fig. 7. Typical time-resolved phosphorescence anisotropy measurement on Ery B in a dry (solid line) and in a wet (dotted line) PVA film. The concentration of dye in the polymer film was $2*10^{-7}$ mol/g.

DISCUSSION

Phosphorescence and Fluorescence Anisotropy

We measured the time-resolved phosphorescence and steady-state fluorescence anisotropy of Ery B in NC and in PVA. These systems were selected because they proved to be a suitable host for fluorescent dye molecules [20,21,34–36]. It is shown that it is possible to immobilize the dye molecules on the phosphorescence time scale. Furthermore, no differences were found between the NC and PVA films. Exciting at 532 nm, we found the same anisotropies in both systems, $r_{\text{phos.532}} = 0.25 \pm 0.01$ and $r_{\text{fluo.532}} = 0.38 \pm 0.01$. In our experiments we took special care that the spectra of both systems were similar to the spectra of Ery B in glycerol.

In the past different values for the phosphorescence anisotropy of Ery B have been found. Prochniewicz *et al.* [12] and Garland and Moore [16] both used a PMMA matrix to immobilize the dye. The anisotropy they found was, respectively, $r_{\text{phos.532}} = 0.205$ and $r_{\text{phos.532}} = 0.25$. We found (to be published), however, that the MMA polymerization affects the spectral properties of the Ery B and that therefore the anisotropy values of Ery B in PMMA are not to be trusted. Zidovedsky *et al.* [6] and Ludescher and Liu [15] used a glass of DL arabinose to immobilize the dye. They found phosphorescence anisotropies of, respectively, $r_{\text{phos.532}} = 0.21$ and 0.22. In the case of an arabinose glass the differences from our values may be explained by a possibly incomplete immobilization of the dye in the glass. Furthermore, too high excita-

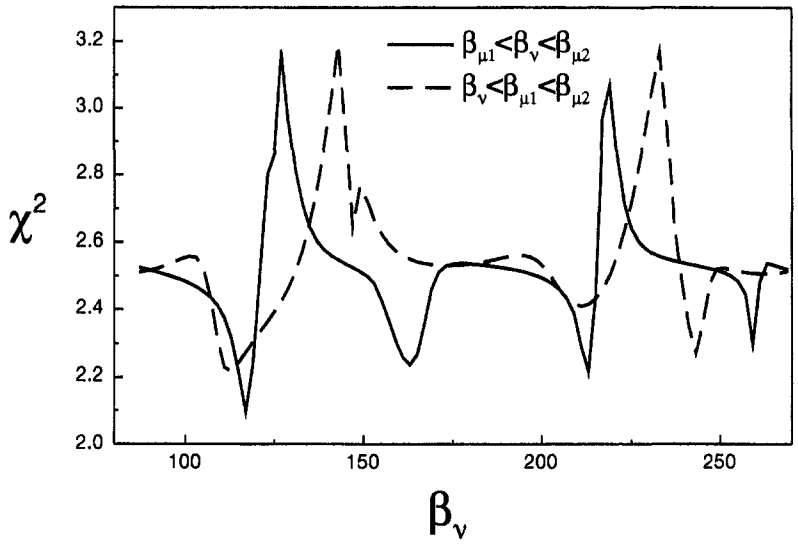

Fig. 8. The χ^2 profile of the AFD fit for $\beta_{\mu1} < \beta_\nu < \beta_{\mu2}$ (solid line) and for $\beta_\nu < \beta_{\mu1} < \beta_{\mu2}$ (dashed line).

tion energies, causing a broadening of the excitation distribution, also might have caused the too low anisotropies in this study [38,39]. Ludescher and Liu [15] also measured the fluorescence anisotropy in glycerol and found a value of 0.385 ± 0.005 for the S_0–S_1 transition, which corresponds reasonably well with our values.

While Pavlopoulos and El Sayed [23] measured excitation anisotropy spectra for various molecules, none of the authors mentioned above did so for Ery B. We show now that information about the anisotropy for excitation at 355 nm is inevitable for the determination of the absolute orientation of the phosphorescence dipole moment.

Combining the fluorescence and phosphorescence anisotropies, two possible orientations of the phosphorescence dipole moment can be calculated, using Eq. (4) and Eq. (7) or (9), depending on the positions of the absorption dipole moments relative to the fluorescence dipole moment. This orientation of the phosphorescence dipole moment can be expressed in the tilt of the phosphorescence dipole moment out of the plane of the molecule, φ_{yz}, and the angle between the projection of the phosphorescence dipole moment in the molecular plane and that of the absorption dipole moment, δ_{xz355} or δ_{xz532}.

In case 1, both the absorption dipole moments being positioned at the same side of the fluorescence dipole moment ($\beta_\nu < \beta_{\mu1} < \beta_{\mu2}$), we find $\varphi_{yz} = 28 \pm 1°$ and $\delta_{xz532} = 9 \pm 3°$, using Eqs. (7) and (4). In case 2, with the fluorescence dipole moment being positioned between the two absorption dipole moments ($\beta_{\mu1} < \beta_\nu < \beta_{\mu2}$), $\varphi_{yz} = 24 \pm 4°$ and $\delta_{xz532} = 16 \pm 2°$, using Eqs. (9) and (4). Thus, in case 2 the projection of the phosphorescence dipole moment is farther away from the absorption dipole moment (and closer to the fluorescence dipole moment) than in case 1. Consequently, having the same total difference angle, in case 2 the phosphorescence dipole moment is tilted out of the molecular plane less than in case 1, 24 vs 28° (see Fig. 2).

The results of the AFD, which we discuss in the next paragraph, will enable us to make a distinction between the possible orientations of the two excitation dipole moments relative to the fluorescence dipole moment, and therefore between the two possible orientations of the phosphorescence dipole moment.

AFD

We have shown in the previous paragraph that the relative orientation of the absorption and fluorescence

Table I. Results of AFD Experiments on Ery B in a Stretched NC film (3× Its Original Length; Concentration, $2 * 10^{-7}$ mol/g)

	1	2	3	4
χ^2	2.10	2.24	2.21	2.40
λ_2	−1.7 ± 0.5	0.6 ± 0.03	3 ± 1	−3 ± 1
λ_4	2.0 ± 0.5	−1.0 ± 0.04	1.0 ± 0.5	−3 ± 1
ε	0.0 ± 0.05	−0.6 ± 0.03	−4 ± 2	−0.1 ± 0.05
β_ν	117	163	213	258

[a] $\beta_{\mu,532} = \beta_\nu - 13°$ and $\beta_{\mu,355} = \beta_\nu + 54°$. The error in the angles is 3°. The error margins are estimated from the broadness of the χ^2 minimum.

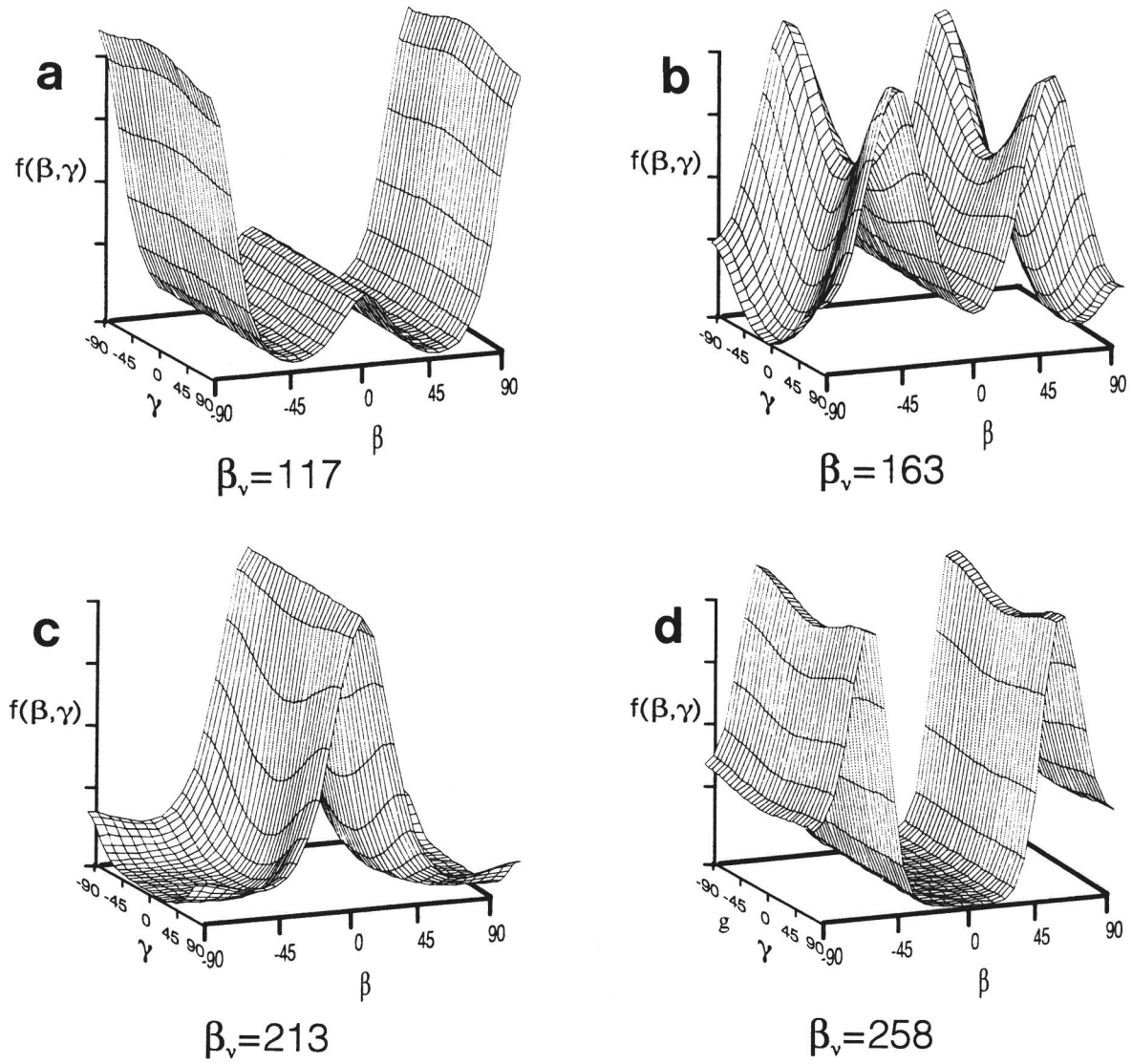

Fig. 9. Orientational distribution functions describing the orientation of Ery B in a stretched PVA film. Functions a to d belong to solutions 1 to 4 as given in Table I. Emission was detected at 573 nm, while excitation was either at 338 nm or at 532 nm.

dipole moments strongly influences the determination of the orientation of the phosphorescence dipole moment. As indicated under Results, solutions were found for $\beta_{\mu 1} < \beta_\nu < \beta_{\mu 2}$ as well as for $\beta_\nu < \beta_{\mu 1} < \beta_{\mu 2}$. However, some features of both types of solutions were clearly different. These differences will enable us to make a choice between them.

The most important difference is that the χ^2 of the $\beta_{\mu 1} < \beta_\nu < \beta_{\mu 2}$ solutions is lower than the χ^2 of the $\beta_\nu < \beta_{\mu 1} < \beta_{\mu 2}$ solutions. Another important check is the consistency between the various solutions of one fit corresponding to minima in the χ^2 profile. If, within one χ^2 profile, two separate orientational distributions functions are peaked around $\beta_1 = 0$ or 90°, this means that solutions are found for two different z-axes which are perpendicular to each other. Therefore a rotation over 90° of the angles β_ν, $\beta_{\mu 1}$, and $\beta_{\mu 2}$ belonging to one solution should yield the angles β_ν, $\beta_{\mu 1}$, and $\beta_{\mu 2}$ belonging to the other solution. For the $\beta_{\mu 1} < \beta_\nu < \beta_{\mu 2}$ solutions, this indeed was the case, while this rotation for the $\beta_\nu < \beta_{\mu 1} < \beta_{\mu 2}$ solutions gave an incoherent picture. Finally, it should also be considered that, because of symmetry [28], the difference angle between the two absorption dipole moments is believed to be close to 90°, which is far from true for $\beta_\nu < \beta_{\mu 1} < \beta_{\mu 2}$.

The orientations of the absorption dipole moments relative to the fluorescence dipole moment are therefore taken to lie on either side of the fluorescence dipole

moment. These findings are in contrast with earlier findings for eosin-5-maleimide [20] but in correspondence with the findings for 5-iodoacetamidetetramethylrhodamine by van Zandvoort *at al.* [22]. The reason for the discrepancy might be found in the fact that van der Heide *et al.* [20] took the anisotropy for eosine-5-maleimide to be constant in the blue region, which is certainly not correct for Ery B (see Fig. 6) and 5-iodoacetamidetetramethylrhodamine. Our calculations on the molecular structure show (Fig. 10) that the xanthene ring structure indeed is planer, so that we can take the transition dipole moments to lie in this plane. The additional phenyl ring is not in the same plane as the xanthene ring, but it does not belong to the chromophore.

Having answered the question of the relative orientations of the absorption and fluorescence dipole moments, the remaining problem is to find the orientations of these transition dipole moments within the molecular frame. In Table I the solutions corresponding to $\beta_{\mu 1} < \beta_{\nu} < \beta_{\mu 2}$ are given for the fit of one measured sample. Each solution contains the distribution function of a chosen molecular z-axis relative to the stretching direction in the film and the orientations of the transition dipole moments relative to this z-axis.

Interpreting the solutions, the molecular z-axis has to be related to the inertial axis of the molecule. This has been done on the basis of calculations of the molecular structure. These calculations show that Ery B has a main inertial axes (axis I in Fig. 10), which is localized within 3° of the long axis of the xanthene ring structure, and a second axis perpendicular to the main axis (axis II). The eigen value, belonging to axis I is a factor 2 higher than the eigen value belonging to axis II. Thus, upon stretching the polymer film, the embedded dye will be oriented in two preferential directions. This compares nicely with

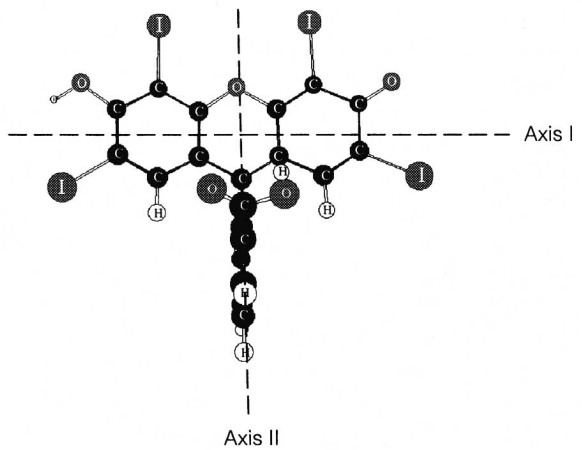

Fig. 10. Calculated structure of Ery B, with inertial axes.

the orientational distribution functions depicted in Fig. 9. The orientational distribution function belonging to solution c has a clear maximum around $\beta = 0$, while small wings are found at $\beta = \pm 90°$, $\gamma = \pm 90°$. This implies that the choice of the molecular z-axis should be such that this axis preferentially aligns parallel to the stretching axis, while a small probability remains for orientation of this axis perpendicular to the stretching direction. It is thus logical to relate this choice of molecular z-axis to the longest of the two inertial axes of Ery B, being axis I. The angles of the transition dipole moments, belonging to solution c, are given relative to this inertial axis. Clearly, the solution indicated in Fig. 9a, corresponds to the choice of the molecular z-axis perpendicular to the inertial axis chosen in solution c, being axis II. The orientational distribution function of the z-axis belonging to solution a can indeed be related to the orientational distribution function of the z-axis belonging to solution c by a rotation of the axis over 90°. The z-axis belonging to solutions b and c lies between axis I and axis II at 48 and 55°, respectively. The distribution functions of solutions b and d are forced to be symmetric around $\beta = 0$, because it is impossible to gain odd order parameters from this experiment. Therefore the χ^2 of these solutions is higher and the S_{μ}, S_{ν}, and G_k differ from the other solutions.

Once the inertial axes are localized in the molecular frame, the transition dipole moments can be placed within the plane of the xanthene ring structure. Taking $\beta_{\mu 1} < \beta_{\nu} < \beta_{\mu 2}$, we find that the S_0–S_1 dipole moment $\vec{\mu}_{532}$ is localized at 18 ± 5° from the axis I of the xanthene ring structure and that the fluorescence dipole moment $\vec{\nu}_{flu}$ is localized at 31 ± 5° from this axis. This corresponds with previous findings [20,22], although the tilt from axis I is more than expected. The fact that $\vec{\mu}_{532}$ and $\vec{\nu}_{flu}$ are not parallel has already been found for other molecules [20,21] and explained [2]. The orientation of the effective 338-nm absorption dipole moment $\vec{\mu}_{355}$ is −3 ± 5° from the short axis of the xanthene part (axis II). Since the anisotropy at 338 nm is about the same as the anisotropy at 355 nm, we believe that the effective dipole moment at 355 nm also has the same orientation as the 338 nm dipole moment. The results are depicted in Fig. 11. The difference angle between the two absorption dipole moments, $\Delta\mu$ ($= \varepsilon_{532} + \varepsilon_{355}$), equals 68°. In the minimum of the anisotropy, around 310 nm (see Fig. 6), we find $\varepsilon_{310} = 63°$, which makes $\Delta\mu$ equal to 76°. This absorption dipole moment is therefore positioned 5° at the other side of axis II. The error margins in the orientations of the transition dipole moments were determined considering the statistical errors in measurements on different samples. The errors determined thus appear to be somewhat

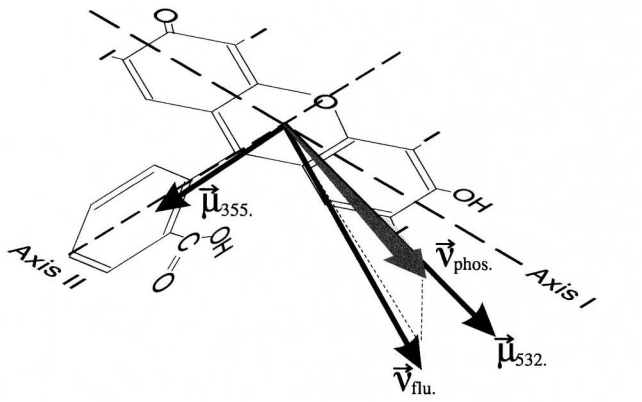

Fig. 11. Orientation of the transition dipole moments within the molecular frame, as deduced from AFD and TPA experiments.

larger than the errors determined from the broadness of the minimum in the χ^2 profile within one measurement. All measurements showed similar distribution functions, but depending on the film, and thus on the stretching amount, different ordering was found. The error margins in the order parameters did not effect the shape of the distribution functions.

Combining AFD with TPA

One of the main features of the AFD technique is that an unequivocal orientation of the transition dipole moments in the molecular frame can be found. We found that the fluorescence dipole moment is located between the two absorption dipole moments, $\beta_{\mu 1} < \beta_{\nu} < \beta_{\mu 2}$. This compares with case 2 as mentioned under Theory and shown in Fig. 2b. Now the phosphorescence dipole moment can be positioned within the molecular frame. This orientation is given by the tilt out of the plane, φ_{yz} (already determined to be 24°), and the angle between the projection of $\vec{\nu}_{phos}$ on the xz-plane and the z-axis, φ_{xz}:

$$\varphi_{xz} = \beta_{\mu 532} - \delta_{xz532} \tag{17}$$

which equals 34° (see Fig. 11).

In earlier studies [16] the difference angle between the 532-nm absorption dipole moment and the phosphorescence dipole moment, as obtained from only phosphorescence anisotropy experiments, was interpreted as a direct tilt out of the molecular plane. However, with $\beta_{\mu 1} < \beta_{\nu} < \beta_{\mu 2}$, the phosphorescence dipole moment is located above the fluorescence dipole moment and *not* above the absorption dipole moment. Since the latter two dipole moments are not parallel, this induces an extra difference angle between the absorption and the phosphorescence dipole moments, which in the past has been interpreted erroneously as an extra tilt out of the plane. Therefore the tilt out of the plane of the molecule is 5° less than expected in the studies mentioned.

CONCLUSION

The AFD results indicate that the halogenation affects the position of the absorption and fluorescence dipole moments. The shift of the 532-nm absorption dipole moment and of the fluorescence dipole moment relative to the long axis of the xanthene ring was more than that found for rhodamine derivatives [22] and eosin-5-maleimide [20]. On the other hand, the 310-nm absorption dipole moment remains aligned along the short axis of the xanthene ring. These findings suggest that the S_0–S_1 transition is perturbed by the halogenation, whereas the S_0–S_2 transition is left unaffected.

As early as the sixties it was suggested that for various phosphorescent molecules, the phosphorescence dipole moment is tilted out of the molecular plane [23]. The addition of heavy atoms appeared to have a strong influence on both the phosphorescence quantum yield and the tilt of the phosphorescence dipole moment. This was explained in terms of the spin–orbital coupling [16]. Here, we have presented a method to determine the orientation of the phosphorescence dipole moment within the molecular plane, combining AFD measurements with the determination of the phosphorescence anisotropies at two excitation wavelengths. We have applied this method to Ery B, a tetraiodo derivative of fluorescein, and found that indeed the phosphorescence dipole moments is tilted out of the plane of the molecule. We have, furthermore, shown that the tilt is less than expected from just the anisotropy measurements [16]. The reason for this difference is that, in general, the difference angle between the S_0–S_1 absorption dipole moment and the phosphorescence dipole moment is directly taken as the tilt of the phosphorescence dipole moment out of the plane of the molecule. In contrast, our results show that the phosphorescence dipole moment is located above the fluorescence dipole moment and *not* above the absorption dipole moment.

In principle, the orientation of the phosphorescence dipole moment could have been found, performing angle-resolved phosphorescence depolarization measurements. However, this experiment has a few drawbacks. First, the tilt of the phosphorescence dipole moment out of the plane introduces extra fit parameters. Since we already needed to cut back the amount of fit parameters, this is an unwelcome feature. Measuring the fluorescence and phosphorescence sequentially could resolve this problem but would be a difficult experiment to perform. Second, the absolute intensity of the emitted light under most

angles is very low. This makes the fluorescence experiment difficult to perform, but the phosphorescence experiment nearly impossible, since the phosphorescence quantum yield is significantly lower that the fluorescence quantum yield. We have shown that with a combination of AFD and TPA experiments, these problems can be circumvented.

The knowledge of the orientation of the phosphorescence dipole moment within the molecular frame of Ery B can now be used in the interpretation of TPA experiments on (biological) systems. In the future we will apply the same combination of techniques on molecules with two iodine atoms instead of four, and bromine atoms instead of iodine. In this way we hope to gain a better understanding of the influence of halogenation on the orientation of the transition dipole moments. More importantly, we then have a variety of fully characterized phosphorescence dye molecules, which can be applied in the study of rotational dynamics on the micro- to millisecond time scale.

ACKNOWLEDGMENTS

The authors would like to thank Dr. E. L. de Beer, Department of Medical Physiology and Sports Medicine, Utrecht University, for the use of the Nd:YAG laser system.

NOMENCLATURE

$\vec{\mu}_{355,532}$	Absorption dipole moments for excitation at 355 and 532 nm, respectively
$\vec{\nu}_{flu,phos}$	Emission dipole moment for the fluorescence and phosphorescence, respectively
$\epsilon_{355,532}$	Angle between the respective absorption dipole moments and the fluorescence dipole moment
$\delta_{532,532}$	Angle between the respective absorption dipole moments and the phosphorescence dipole moment
$\Delta\mu$	Difference angle between the two absorption dipole moments
$\delta_{xz355,532}$	Angle between the respective absorption dipole moments and the projection of the phosphorescence dipole moment on the *xz*-plane
φ_{yz}	Angle between the projection of $\vec{\nu}_{phos.}$ on the *yz*-plane and the *z*-axis
φ_{xz}	Angle between the projection of $\vec{\nu}_{phos.}$ on the *xz*-plane and the *z*-axis

REFERENCES

1. J. R. Lakowicz (1983) *Principles of Fluorescence Spectroscopy*, Plenum Press, New York.
2. Y. K. Levine and G. van Ginkel (1994) in G. R. Luckhurst and C. A. Veracini (Eds.), *The Molecular Dynamics of Liquid Crystals*, Kluwer Academic, Dordrecht, pp. 537–571.
3. E. Grell (1981) *Membrane Spectroscopy*, Springer-Verlag, Berlin.
4. S. C. Hopkins, C. Sabido-David, J. E. T. Corrie, M. Irving, and Y. E. Goldman (1998) *Biophys. J.* **74**, 3093–3110.
5. R. J. Cherry and G. Schneider (1976) *Biochemistry* **15**, 3657–3661.
6. R. Zidovetski, M. Bartholdi, D. Arndt-Jovin, and T. M. Jovin (1986) *Biochemistry* **25**, 4397–4401.
7. A. M. Rubtsov, A. A. Boldyrev, L. Yang, D. McStay, and P. J. Quinn (1994) *Biochemistry* **59**, 1263–1268.
8. D. A. Roess, M. A. Jewell, C. J. Philpott, and B. G. Barisas (1997) *Biochim. Biophys. Acta* **1375**, 98–106.
9. R. D. Ludescher and D. D. Thomas (1988) *Biochemistry* **27**, 3343–3351.
10. R. A. Stein, R. D. Ludescher, S. Dahlberg, P. G. Fajer, L. H. Bennet, and D. D. Thomas (1990) *Biochemistry* **29**, 10023–10031.
11. D. D. Thomas, S. Ramachandran, O. Roopnarine, D. W. Hayden, and E. M. Ostap (1995) *Biophys. J.* **68**, 135s–141s.
12. E. Prochniewicz, Q. Zhang, E. C. Howard, and D. D. Thomas (1996) *J. Mol. Biol.* **225**, 446–457.
13. H. Yoshimura, T. Nishio, K. Mihashi, K. Kinosita Jr., and A. Ikegami (1984) *J. Mol. Biol.* **179**, 453–467.
14. W. H. Sawyer, A. G. Woodhouse, J. J. Czarnecki, and E. Blatt (1988) *Biochemistry* **27**, 7733–7740.
15. R. D. Ludescher and Z. Liu (1993) *Photochem. Photobiol.* **58**, 858–866.
16. P. B. Garland and C. H. Moore (1979) *Biochem. J.* **183**, 561–572.
17. U. A. van der Heide, O. E. Rem, H. C. Gerritsen, E. L. de Beer, P. Schiereck, I. P. Trayer, and Y. K. Levine (1994) *Eur. Biophys. J.* **23**, 369–378.
18. M. van Gurp, H. van Langen, G. van Ginkel, and Y. K. Levine (1988) in B. Samori and E. W. Thulstrup (Eds.), *Polarized Spectroscopy of Ordered Systems*, Kluwer Academic, Dordrecht, pp. 455–489.
19. M. van Gurp and Y. K. Levine (1989) *J. Chem. Phys.* **8**, 4095–4102.
20. U. A. van der Heide, B. Orbons, H. C. Gerritsen, and Y. K. Levine (1994) *Eur. Biophys. J.* **21**, 263–272.
21. M. A. M. J. van Zandvoort, D. Wróbel, P. Lettinga, G. van Ginkel, and Y. K. Levine (1995) *Photochem. Photobiol.* **62**, 299–308.
22. M. A. M. J. van Zandvoort, D. L. J. Vossen, G. van Ginkel, R. Torre, P. Bartolini, M. Ricci, J. Thomas-Oates, and H. Zuilhof, submitted.
23. T. Pavlopoulos and M. A. El Sayed (1964) *J. Chem. Phys.* **64**, 1082–1092.
24. M. van Gurp, Y. K. Levine, and G. van Ginkel (1998) *J. Polym. Sci. B* **26**, 1613.
25. C. Zannoni, A. Arcioni, and P. Cavartorta (1983) *Chem. Phys. Lipids* **32**, 323.
26. Ph. Wahl (1983) in R. B. Cundall and R. E. Dale (Eds.), *Time-Resolved Fluorescence Spectroscopy in Biochemistry and Biology*, Plenum Press, New York, pp. 483–522.
27. J. Szubiakowski, A. Balter, W. Nowak, A. Kowalczyk, K. Wisniewski, and M. Wierzbowska (1996) *Chem. Phys.* **208**, 283–296.
28. L. B. A. Johansson and A. Niemi (1987) *J. Phys. Chem.* **91**, 3020.
29. M. E. Rose (1957) *Elementary Theory of Angular Momentum*, Wiley, New York.
30. M. van Gurp and Y. K. Levine (1991) *Chem. Phys. Lett.* **180**, 349.
31. Particle Data Group (1976) *Rev. Mod. Phys.* **48**, s36.
32. J. Arden, G. Deltau, V. Huth, U. Kringel, D. Peros, and K. H. Drexhage (1991) *J. Luminesc.* **48/49**, 352.
33. R. D. Levine and R. B. Bernstein (1975) in W. H. Miller (Ed.), *Modern Theoretical Chemistry, Vol. III. Dynamics of Molecular Collisions*. Plenum, New York.

34. M. A. M. J. van Zandvoort, D. Wróbel, A. J. Scholten, D. de Jager, G. van Ginkel, and Y. K. Levine (1993) *Photochem. Photobiol.* **58**, 600–606.
35. M. A. M. J. van Zandvoort, D. Wróbel, P. Lettinga, G. van Ginkel, and Y. K. Levine (1995) *Photochem. Photobiol.* **62**, 279–289.
36. D. Wróbel, M. A. M. J. van Zandvoort, P. Lettinga, G. van Ginkel, and Y. K. Levine (1995) *Photochem. Photobiol.* **62**, 290–298.
37. Y. Nashijima, Y. Onogi, R. Yamazaki, and K. Kawakami (1968) *Rep. Prog. Polym. Phys. Jpn.* **11**, 407–410.
38. H. Peng and B. G. Barisas (1997) *J. Fluoresc.* **7**, 139–145.
39. J. R. Lakowicz, I. Gryczynski, V. Bogdanov, and J. Kusba (1994) *J. Phys. Chem.* **98**, 334–342.
40. J. R. Herman, T. R. Londo, N. A. Rahman, and B. G. Barisas (1992) *Rev. Sci. Instrum.* **63**, 5454–5458.
41. L. Yang, D. McStay, A. J. Rogers, and P. J. Quinn (1993) *Opt. Eng.* **32**, 354–360.
42. S. G. Ballard (1983) *Rev. Sci. Instrum.* **54**, 1473–1475.
43. (a) J. J. P. Stewart (1989) *J. Comp. Chem.* **10**, 209–220; (b) J. J. P. Stewart (1989) *J. Comp. Chem.* **10**, 221.
44. J. J. P. Stewart (1993) *MOPAC93*, Fujitsu,Tokyo.